Brownian dynamics and dynamic Monte Carlo simulations of isotropic and liquid crystal phases of anisotropic colloidal particles: A comparative study

Alessandro Patti[1,*] and Alejandro Cuetos[2,†]

[1]*Institute of Advanced Chemistry of Catalonia (IQAC-CSIC) and CIBER de Bioingeniería, Biomateriales y Nanomedicina (CIBER-BBN), Jordi Girona 18-26, 08034 Barcelona, Spain*

[2]*Department of Physical, Chemical, and Natural Systems, Universidad Pablo Olavide, 41013 Sevilla, Spain*

(Received 23 April 2012; revised manuscript received 14 June 2012; published 9 July 2012)

We report on the diffusion of purely repulsive and freely rotating colloidal rods in the isotropic, nematic, and smectic liquid crystal phases to probe the agreement between Brownian and Monte Carlo dynamics under the most general conditions. By properly rescaling the Monte Carlo time step, being related to any elementary move via the corresponding self-diffusion coefficient, with the acceptance rate of simultaneous trial displacements and rotations, we demonstrate the existence of a unique Monte Carlo time scale that allows for a direct comparison between Monte Carlo and Brownian dynamics simulations. To estimate the validity of our theoretical approach, we compare the mean square displacement of rods, their orientational autocorrelation function, and the self-intermediate scattering function, as obtained from Brownian dynamics and Monte Carlo simulations. The agreement between the results of these two approaches, even under the condition of heterogeneous dynamics generally observed in liquid crystalline phases, is excellent.

DOI: 10.1103/PhysRevE.86.011403 PACS number(s): 82.70.Dd, 61.30.−v, 87.15.Vv

I. INTRODUCTION

The dynamics of colloidal particles are well described by the classical theory of Brownian motion [1], named after the botanist Robert Brown who, in 1827, observed organelles suspended in water performing persistent and casual jumpy moves [2]. Briefly speaking, the Brownian motion is due to the random collisions between suspended colloidal particles and the molecules of the fluid surrounding them. Because of this random drifting, colloidal systems are very good candidates to be described via Brownian dynamics (BD) or Monte Carlo (MC) simulations. In both methods, a stochastic rather than deterministic approach is applied. More specifically, in BD simulations stochastic differential equations are solved to describe the time-evolution of suspended particles under the effect of thermal fluctuations. By contrast, in MC simulations, a sequence of random numbers is generated to make the particles perform random walks in the space of configurations: their moves are accepted with a given transition probability satisfying the condition of detailed balance [3,4].

In the past few years, there has been a growing interest in the field of molecular simulation on applying stochastic algorithms to investigate the dynamics of equilibrium and out-of-equilibrium colloidal fluids, such as liquid crystals and supercooled liquids, respectively. In particular, the high efficiency of the MC technique allowed to handle the significantly long relaxation dynamics of glass-forming systems [5,6] and liquid crystals [7–11], to study the crystal nucleation rate in hard-sphere colloids [12], and the dynamics of several self-assembling systems [13–16]. These studies did not limit the application of the MC method to systems of hard particles, where the molecular dynamics (MD) or BD approaches cannot be straightaway implemented, but extended to systems of particles interacting via a soft potential, where MD or BD should be the most appropriate choice. In these studies, the MC simulation method is usually referred to as dynamic MC (DMC). More precisely, the DMC technique is based on the standard Metropolis algorithm, where any new state of the system stems from the former one according to a probability which depends on the energy jump between the two states [17]. Strictly speaking, this nondeterministic progression of states follows a time-independent path through the phase space. However, in the limit of very small displacements, where configurational biased moves, cluster moves, swaps, or other unphysical moves are not allowed, Metropolis-based DMC simulations may mimic the Brownian motion of particles and describe time-dependent processes. The application of the MC method to investigate the Brownian evolution of a given colloidal system implies (i) to define a unique MC time scale being independent from the size of the MC change of any degree of freedom; and (ii) to relate such an MC time scale to the BD time scale. Addressing these two crucial aspects is fundamental to correctly compare both simulation methods on a quantitative basis.

Recently, Sanz and coworkers have proposed an algorithm to mimic the Brownian dynamic with DMC simulations. These authors reported on comparative studies between DMC and BD in the isotropic phase of smooth and patchy spherical particles [18,19]. In their most general scenario, where translational and rotational degrees of freedom are involved, they performed DMC simulations by attempting, on average, N rotations and N translations in each cycle, with N the number of particles in the system. This scheme generates two distinct values of the acceptance rate, one for translations (a_t) and another for rotations (a_r), which clearly depend on the maximum translation (δ_t) and rotation (δ_r) allowed. In order to map DMC into BD, these authors showed that the following condition, where the Einstein and Stokes-Einstein relations are involved, must hold $3\delta_t/\delta_r = \sigma\sqrt{a_r/a_t}$, with σ the particle diameter

*alpnqb@iqac.csic.es
†acuemen@upo.es

[19]. A trial-and-error iterative procedure, consisting of few short preliminary simulations, is recommended in order to fix the value of δ_t and δ_r satisfying this *a priori* requirement.

In the present work, we introduce an alternative DMC algorithm for particles with arbitrary degrees of freedom, which does not make use of any preliminary simulation and therefore bypasses the trial and error procedure described in Refs. [18,19]. In order to check the validity of our approach, we compared few dynamic properties computed by performing DMC and BD simulations in liquid crystalline phases of colloidal rod-like particles. In such systems, the diffusion along the nematic director and that in the plane perpendicular to it are significantly different, and therefore imply distinct maximum displacements while maintaining a common time scale. Particles are displaced and rotated simultaneously and a single value of the acceptance rate is therefore generated. The acceptance rate represents the scaling factor relating the time scales of BD and DMC simulations. To introduce the concept of MC time, we make use of the Einstein relations, linking any elementary move with the MC time step via the corresponding diffusion coefficients [20]. By rescaling any MC time step by this acceptance rate, we obtain a unique MC time scale which does not depend on the maximum displacements and rotations. Regardless of the dynamic properties discussed here, the rescaled results of DMC simulations collapse on a single master curve and are in excellent agreement with the results of BD simulations at high acceptance rates, being still very satisfactory at those acceptances usually required in standard MC simulations.

This paper is organized as follows. In Sec. II, we describe the theoretical framework applied to compare the two stochastic approaches. In Sec. III, the model and methodology to perform BD and DMC simulations are presented. In Sec. IV, we discuss our results by focusing on the qualitative and quantitative agreement between BD and DMC. Finally, some conclusions wrap up the paper.

II. THEORY

In this section, we investigate the link between the evolution of a system of particles in Brownian motion and in MC dynamics. To this end, it is key to establish a consistent and rigorous time scale being independent from the acceptance rate of DMC simulations. For the sake of clarity, the trivial case of a system with only one degree of freedom is first discussed. Let's consider a particle j originally located at $x = 0$. In a standard MC scheme, where unphysical moves are not allowed, j can be displaced to a new randomly selected position in the interval $[-\delta x,\delta x]$. According to the Metropolis algorithm, the probability to accept this move depends on the interactions established by particle j in the old and new configuration of the system. More specifically, this probability is a function of the size of the displacement: the shorter the displacement, the higher the probability to accept the move.

Here, we assume that this acceptance probability does not depend on the step size of displacement, but remains constant in the interval $[-\delta x,\delta x]$. The validity of this crucial assumption might be significantly affected at high concentrations and/or when the interactions between particles become stronger. In these cases, the acceptance rate might be strongly dependent on the step size of displacement and hence a very small time step would be required in order to obtain a satisfactory approximation. However, in the limit of infinite dilution as well as at infinitely small displacements, exact results are expected. This level of approximation is equivalent to that employed in [18] for the 1D case, where an expansion up to first order of the force exerted over the particle as function of the displacement was considered. Under this approximation, the probability of finding a particle in its original position after a rejected trial move is defined as $P_{\text{reject}} = \mathcal{A}'$. Accordingly, the probability to accept the move is $P_{\text{accept}} = 1 - \mathcal{A}' = \mathcal{A}$. The normalized probability to successfully move a particle to the position $x \in [-\delta x,\delta x]$ is $P_{\text{move}} = \mathcal{A}/2\delta x$, being the general solution to the problem of random walk with hesitation [21]. Therefore, the mean displacement reads $\langle x\rangle = \int_{-\delta x}^{\delta x} x\,P_{\text{move}}dx = 0$, as expected for Brownian motion of suspended colloids. Whereas, the mean square displacement, limited to a single MC step, reads

$$\langle x^2\rangle = \int_{-\delta x}^{\delta x} x^2\,P_{\text{move}}dx = \frac{\mathcal{A}(\delta x)^2}{3}. \tag{1}$$

In an MC step, we attempt to move a randomly selected particle in the interval $[-\delta x,\delta x]$. It is straightforward to extend this result to a system of N particles performing $\mathcal{C}_{\text{MC}}$ cycles, being a cycle equal to N statistically independent MC steps. In this case, the mean square displacement reads

$$\langle x^2\rangle = \mathcal{C}_{\text{MC}}\frac{\mathcal{A}(\delta x)^2}{3}, \tag{2}$$

where $\mathcal{A}$ is again the probability to accept the move for each MC step.

In a 3D space, the number of degrees of freedom increases to five for particles with axial symmetry: three of them are associated with the displacement of the center of mass of the particles, and the remaining two with their rotation. Here, we discuss the most general case of f degrees of freedom. A given particle is moved from the origin to a point $\xi = (\xi_1,\xi_2,\ldots,\xi_f)$ belonging to an f-dimensional hyperprism of sizes $[-\delta\xi_k,\delta\xi_k]$, with $k = 1,2,\ldots,f$. As in the $f = 1$ case, it is supposed that this move can be accepted with a uniform probability $\mathcal{A}$ independent on the displacement. Hence, the normalized probability of a successful displacement of a particle to any point inside this interval reads

$$P_{\text{move}}(\xi) = \frac{\mathcal{A}}{V_\Xi}, \tag{3}$$

where $V_\Xi = \prod_i^f (2\delta\xi_k)$ is the volume of the hyperprism defined above. As obtained for the 1D case, the expected value of the mean displacement is $\langle\xi_k\rangle = 0$ for any degree of freedom $k \leqslant f$. By contrast, the mean square displacements take the following form:

$$\langle\xi_k^2\rangle = \int_{V_\Xi} \xi_k^2\,P_{\text{move}}d\xi_k = \frac{\mathcal{A}(\delta\xi_k)^2}{3}. \tag{4}$$

It should be noticed that this result is independent on the number of degrees of freedom. This might not be the case if the acceptance probability could not be considered uniform in the f-dimensional hyperprism. Again, it is straightforward to extend this result to the case of N identical particles performing

$\mathcal{C}_{\mathrm{MC}}$ cycles. In this case, the mean square displacement reads

$$\langle \xi_k^2 \rangle = \mathcal{C}_{\mathrm{MC}} \frac{\mathcal{A}(\delta\xi_k)^2}{3}. \tag{5}$$

This result allows us to define a time unit for a DMC simulation (t_{MC}), which can be easily related to the time unit of a BD simulation (t_{BD}). An MC step consists of an attempt to simultaneously modify all the degrees of freedom of a randomly selected particle. Eventually, this attempted move is accepted with a probability $\mathcal{A}$. An efficient way to relate the displacements and rotations of a particle to a temporal scale in a self-consistent way is through the Einstein relation (the same as the Langevin equation at long times) [20]. If the MC moves are statically independent, time and space are related through the self-diffusion coefficient. Hence, an MC time step could be defined through the equation $(\delta\xi_k)^2 = 2D_k\delta t_{\mathrm{MC}}$, where D_k is the self-diffusion coefficient associated to the kth degree of freedom and δt_{MC} is the time needed to perform an MC cycle in the MC timescale. By combining this result with Eq. (5), the following expression is obtained:

$$\langle \xi_k^2 \rangle = \tfrac{2}{3}\mathcal{A}D_k\mathcal{C}_{\mathrm{MC}}\delta t_{\mathrm{MC}}. \tag{6}$$

The Einstein relation for a BD simulation reads

$$\langle \xi_k^2 \rangle = 2D_k t_{\mathrm{BD}}. \tag{7}$$

By substituting Eq. (6) in Eq. (7), a relation between both timescales is obtained:

$$t_{\mathrm{BD}} = \frac{\mathcal{A}}{3}\mathcal{C}_{\mathrm{MC}}\delta t_{\mathrm{MC}}. \tag{8}$$

This equation provides a relation between the timescales in BD and DMC simulations. It should be noticed that Eqs. (6)–(8) are exact only at infinite dilution, a limit where the acceptance rate can be considered independent on the size of displacement. By contrast, at finite dilution, due to the collisions between particles, these equations are not exact and give approximated results. $\mathcal{A}$ is strictly related to the complete set of $\delta\xi_k$, which depend, in turns, on the MC time unit δt_{MC} as defined above. Distinct values of δt_{MC} furnish a unique MC timescale, equal to the BD timescale, when scaled by the corresponding acceptance rate $\mathcal{A}$. In other words, Eq. (8) establishes a unique timescale for DMC simulations, given the definition of MC step provided above.

The question that arises here is how small the maximum displacements $\delta\xi_k$ should be. As already mentioned, we are supposing that the acceptance ratio $\mathcal{A}$ is independent on the displacement and uniform in the hyperprism of sizes $[-\delta\xi_k,\delta\xi_k]$. This assumption is not compatible with a large time step δt_{MC}. However, although a small δt_{MC} is necessary to ensure the equivalence between DMC and BD simulation, this should not be excessively small to collect significant statistics in an acceptable period of simulation time. Apart from an overall rescaling of the time lengths, any appropriate and efficient selection of displacements and rotations should not affect the dynamics of the system at long time scales, as we demonstrate in this paper.

III. MODEL AND SIMULATION METHODOLOGY

We studied pure systems of rod-like particles containing $N = 1000$ freely rotating spherocylindrical rods with aspect ratio $L^* = L/\sigma = 5$, where L and σ are, respectively, the length and diameter of a cylinder capped by two hemispheres with diameter σ. Particles interact via a shifted and truncated Kihara potential [22,23], which assumes a mere repulsive form:

$$U_{ij} = \begin{cases} 4\epsilon\left[\left(\frac{\sigma}{d_m}\right)^{12} - \left(\frac{\sigma}{d_m}\right)^{6} + \frac{1}{4}\right] & d_m \leqslant \sqrt[6]{2}\sigma \\ 0 & d_m > \sqrt[6]{2}\sigma, \end{cases} \tag{9}$$

where $U_{ij} = U_{ij}(\mathbf{r}_{ij},\hat{\mathbf{u}}_i,\hat{\mathbf{u}}_j)$. The subscripts i and j refer to a pair of interacting particles: $\mathbf{r}_{ij}$ is their center-to-center distance, $\hat{\mathbf{u}}_i$ and $\hat{\mathbf{u}}_j$ their orientations, ϵ the strength of their interaction, and $d_m = d_m(\mathbf{r}_{ij},\hat{\mathbf{u}}_i,\hat{\mathbf{u}}_j)$ the minimum distance between them. For more details on the computation of the minimum distance between two spherocylinders, we refer the interested reader to Ref. [24]. We use σ, ϵ, and $\tau = \sigma^2/D_0$ as length, energy, and time units, respectively, with $D_0 = k_BT/(\mu\sigma)$ a diffusion constant and μ the viscosity coefficient of the solvent [25].

With these general characteristics, we performed DMC and BD simulations in several mesophases. For isotropic (I), nematic (Nm), and smectic (Sm) phases, we set $T^* = k_BT/\epsilon = 20.0, 5.0$, and 3.0, respectively, with k_B the Boltzmann constant and T the absolute temperature. Additionally, the packing fractions are equal to $\eta = 0.490$ in the I and Nm phases, and $\eta = 0.556$ in the Sm phase. To limit the finite size effects, periodic boundary conditions have been applied. To equilibrate the system, long standard MC simulation in the NVT ensemble were carried out. The systems were considered at equilibrium when the total energy, U/ϵ, achieved a steady value within the statistical fluctuations. For each phase of interest, a given equilibrated configuration was chosen as the initial one for all the production runs.

A. DMC simulations

In the production runs, DMC simulations have been performed in the NVT ensemble, with simultaneous attempts to displace and rotate random selected particles. More specifically, translational and rotational moves were accepted according to the standard Metropolis algorithm, that is with probability $\min[1, \exp(-\Delta U/k_BT)]$. If the move is accepted, the total energy of the system is increased by the amount ΔU. To properly mimic the Brownian dynamics of the colloids, no unphysical moves, such as swaps or cluster moves, were performed. For the displacement of the center of mass of a given particle j, the motion is decoupled into three terms: $\delta\mathbf{r}_j = X_{||}\hat{\mathbf{u}}_j + X_{\perp,1}\hat{\mathbf{v}}_{j,1} + X_{\perp,2}\hat{\mathbf{v}}_{j,2}$, where $\hat{\mathbf{u}}_j$ is the orientation vector, and $\hat{\mathbf{v}}_{j,m}$, with $m = 1$ or 2, are two randomly chosen vectors perpendicular to each other and to $\hat{\mathbf{u}}_j$. In each direction, the magnitude of the displacement is chosen at random with the conditions $|X_{||}| \leqslant \delta r_{||}$ and $|X_{\perp,m}| \leqslant \delta r_{\perp}$. For the rotations, the orientation vector of particle j changes from $\hat{\mathbf{u}}_j$ to $\hat{\mathbf{u}}_j + \delta\hat{\mathbf{u}}_j$ with $\delta\hat{\mathbf{u}}_j = Y_{\vartheta,1}\hat{\mathbf{w}}_{j,1} + Y_{\vartheta,2}\hat{\mathbf{w}}_{j,2}$. Again, $\hat{\mathbf{w}}_{j,m}$ are two randomly chosen vectors perpendicular to each other and to $\hat{\mathbf{u}}_j$. The random numbers $Y_{\vartheta,j}$ are chosen in the interval $[-\delta\vartheta,\delta\vartheta]$, where $\delta\vartheta$ is the elementary rotation of

the long axis of the rods. This scheme satisfies the balance condition, as shown in the Appendix. The Einstein relation links the displacements and the rotations to the respective self-diffusion coefficients via the time step δt_{MC}:

$$\delta r_{\perp} = \sqrt{2D_{\perp}\delta t_{\mathrm{MC}}}, \tag{10}$$

$$\delta r_{\parallel} = \sqrt{2D_{\parallel}\delta t_{\mathrm{MC}}}, \tag{11}$$

$$\delta \vartheta = \sqrt{2D_{\vartheta}\delta t_{\mathrm{MC}}}. \tag{12}$$

With regard to the translational and rotational self-diffusion coefficients, we have applied the analytical expressions available for prolate spheroids [26,27]. In particular:

$$D_{\perp} = D_0 \frac{(2a^2 - 3b^2)S + 2a}{16\pi(a^2 - b^2)} b, \tag{13}$$

$$D_{\parallel} = D_0 \frac{(2a^2 - b^2)S - 2a}{8\pi(a^2 - b^2)} b, \tag{14}$$

$$D_{\vartheta} = 3D_0 \frac{(2a^2 - b^2)S - 2a}{16\pi(a^4 - b^4)} b, \tag{15}$$

where $a = L/2$, $b = \sigma/2$, and S is a geometrical parameter given by

$$S = \frac{2}{(a^2 - b^2)^{1/2}} \log \frac{a + (a^2 - b^2)^{1/2}}{b}. \tag{16}$$

Therefore, by fixing a given value for the time step δt_{MC}, the microscopic rotation and displacements listed in Eqs. (10)–(12) are univocally determined. More specifically, in order to ascertain the quality of the comparison between DMC and BD, we performed simulations at time steps $\delta t_{\mathrm{MC}}/\tau = 10^{-4}$, 10^{-3}, 10^{-2}, and $3 \cdot 10^{-2}$. Each time step determines different acceptance rates, as reported in Table I.

It should be noticed that Eqs. (13)–(15) are exact at infinite dilution, that is when the diffusion of a given particle is not hampered by its surrounding neighbors, and all the attempted moves are accepted ($\mathcal{A} = 1$). Increasing the time step implies lower acceptance rates and introduces an approximation in the MC dynamics, as already pointed out in Refs. [18,19], where the optimal translational acceptance rate for systems of patchy spheres was found to be ~ 0.7. This optimal value is a compromise between the efficiency of the MC method and the quantitative agreement with BD simulations. To check the limit of applicability of the DMC method, we have also run simulations at time steps giving acceptance rates $\mathcal{A} \leqslant 0.4$, being the typical interval generally imposed in many standard MC simulations.

B. BD simulations

In a BD simulation, a stochastic differential equation, the so-called Langevin equation, is integrated forward in time and trajectories of particles are created [25,28]. Let's define $\mathbf{r}_j$ as the position of the center of mass of particle j, $\hat{\mathbf{u}}_j$ the unit vector oriented along the long axis of j, $\hat{\mathbf{v}}_{j,m}$ and $\hat{\mathbf{w}}_{j,m}$, with $m = 1$ or 2, two independent pairs of perpendicular unit vectors being also perpendicular to $\hat{\mathbf{u}}_j$. Furthermore, $\mathbf{F}_j$ and $\mathbf{T}_j$ are the total force and torque acting over the particle j. To compute them for systems of particles interacting via a Kihara potential, we refer to Ref. [29]. In a BD step, the position of the center of mass and the orientation of each particle is updated in time by the following set of equations:

$$\mathbf{r}_j^{\parallel}(t + \Delta t) = \mathbf{r}_j^{\parallel}(t) + \frac{D_{\parallel}}{k_B T}\mathbf{F}_j^{\parallel}(t)\Delta t + (2D_{\parallel}\Delta t)^{1/2} R_{\parallel}\hat{\mathbf{u}}_j(t) \tag{17}$$

$$\mathbf{r}_j^{\perp}(t + \Delta t) = \mathbf{r}_j^{\perp}(t) + \frac{D_{\perp}}{k_B T}\mathbf{F}_j^{\perp}(t)\Delta t + (2D_{\perp}\Delta t)^{1/2}[R_1^{\perp}\hat{\mathbf{v}}_{j,1}(t) + R_2^{\perp}\hat{\mathbf{v}}_{j,2}(t)] \tag{18}$$

$$\hat{\mathbf{u}}_j(t + \Delta t) = \hat{\mathbf{u}}_j(t) + \frac{D_{\vartheta}}{k_B T}\mathbf{T}_j(t) \times \hat{\mathbf{u}}_j(t)\Delta t + (2D_{\vartheta}\Delta t)^{1/2}\left[R_1^{\vartheta}\hat{\mathbf{w}}_{j,1}(t) + R_2^{\vartheta}\hat{\mathbf{w}}_{j,2}(t)\right], \tag{19}$$

where $\mathbf{r}_j^{\parallel}$ and $\mathbf{r}_j^{\perp}$ indicate the projections of the positions of particle j along $\hat{\mathbf{u}}_j$ and along the directions perpendicular to $\hat{\mathbf{u}}_j$, respectively; $\mathbf{F}_j^{\parallel}$ and $\mathbf{F}_j^{\perp}$ are the parallel and perpendicular components of the forces, respectively; and $R^{\parallel}, R_1^{\perp}, R_2^{\perp}, R_1^{\vartheta}$, and R_2^{ϑ} are independent Gaussian random numbers of variance

TABLE I. Details of the systems studied in this paper, consisting of spherocylindrical particles (rods) with length to diameter ratio $L^* = L/\sigma = 5$. For comparison, we report the reduced temperature $T^* = k_B T/\epsilon$, packing fractions η, diffusion coefficients $D_{\perp}$, $D_{\parallel}$, and D_{ϑ} in units of σ^2/τ, time step δt_{MC} in units of τ, maximum displacements $\delta r_{\perp}$ and $\delta r_{\parallel}$, in units of σ, maximum rotation $\delta\vartheta$, and acceptance rates $\mathcal{A}$.

	Rods											
Phase	I				Nm				Sm			
T^*	20				5				3			
η	0.490				0.490				0.556			
$D_{\perp}\tau/\sigma^2$	0.793				0.198				0.119			
$D_{\parallel}\tau/\sigma^2$	1.079				0.270				0.162			
$D_{\vartheta}\tau/\sigma^2$	0.175				0.044				0.026			
$\delta t_{\mathrm{MC}}/\tau$	10^{-4}	10^{-3}	10^{-2}	$3 \cdot 10^{-2}$	10^{-4}	10^{-3}	10^{-2}	$3 \cdot 10^{-2}$	10^{-4}	10^{-3}	10^{-2}	$3 \cdot 10^{-2}$
$\delta r_{\perp}/\sigma \cdot 10^2$	1.26	3.99	12.6	21.8	0.631	1.99	6.30	10.9	0.488	1.54	4.88	8.45
$\delta r_{\parallel}/\sigma \cdot 10^2$	1.47	4.65	14.7	25.5	0.735	2.32	7.35	12.7	0.569	1.80	5.69	9.86
$\delta\vartheta \cdot 10^2$	0.837	2.65	8.40	10.3	0.418	1.32	4.18	7.25	0.324	1.02	3.24	5.61
$\mathcal{A}$	0.923	0.757	0.362	0.157	0.955	0.855	0.575	0.356	0.958	0.868	0.609	0.397

1 and zero mean. The diffusion coefficients $D_\parallel$, $D_\perp$, and D_ϑ have been defined in Eqs. (13)–(15). In all BD simulations, the time step was set to $\Delta t = 10^{-4}$.

C. Comparison of simulation techniques

In order to compare the MC dynamics with the Brownian dynamics, some dynamical observables are computed: (i) the mean square displacement (MSD), (ii) the orientation autocorrelation functions (OAF), and (iii) the self part of the intermediate scattering function (ISF). For all the systems studied, we computed the MSD resulting from the displacements along the three axes of the simulation box. It reads:

$$\langle \Delta r^2(t) \rangle = \left\langle \frac{1}{N} \sum_{j=1}^{N} [\mathbf{r}_j(t) - \mathbf{r}_j(0)]^2 \right\rangle, \tag{20}$$

where the delimiters $\langle \ldots \rangle$ denote ensemble average. For systems in the Nm or Sm phase, we also computed the MSD parallel, $\langle \Delta r_\parallel^2(t) \rangle$, and perpendicular, $\langle \Delta r_\perp^2(t) \rangle$, to the nematic director $\hat{\mathbf{n}}$ of the liquid crystalline phase.

The OAF is given by the second Legendre polynomial of the dot product between the unit orientation vectors, $\hat{\mathbf{u}}_j(0)$ and $\hat{\mathbf{u}}_j(t)$, of particle j calculated at time 0 and time t:

$$E_2(t) = \frac{1}{N} \sum_{j=1}^{N} \frac{1}{2} \{ 3 \langle [\hat{\mathbf{u}}_j(0) \cdot \hat{\mathbf{u}}_j(t)]^2 \rangle - 1 \}. \tag{21}$$

The self-ISF gives a measure of the structural relaxation decay of the density fluctuations and reads:

$$F_s(\mathbf{q},t) = \frac{1}{N} \left\langle \sum_{j=1}^{N} \exp\{ i\mathbf{q} \cdot [\mathbf{r}_j(t+t_0) - \mathbf{r}_j(t_0)] \} \right\rangle, \tag{22}$$

where $\mathbf{q} = \mathbf{q}_\perp + \mathbf{q}_\parallel$ is the wave vector calculated at the first peak of the static structure factor in the perpendicular and parallel directions to the nematic director, and $\mathbf{r}_j(t)$ is the particle position at time t. In particular, the transverse and longitudinal relaxations will be given by $F_s^\perp(t) = F_s(q_\perp,t)$ and $F_s^\parallel(t) = F_s(q_\parallel,t)$, respectively.

In order to obtain good statistics in the production of the averaged quantities, all these dynamical observables were averaged over trajectories with multiple time origins.

IV. RESULTS

In this section, we compare the results from DMC and BD simulations in the I, Nm, and Sm phases of rod-like particles. An illustrative configuration for each phase is given in Fig. 1. In the I phase, no long-range order exists and the rods are randomly distributed throughout the simulation box. The Nm phase presents some order in the direction of the rods, which tend to be aligned with a common axis, the nematic director $\hat{\mathbf{n}}$, whose orientation is arbitrary in space. Finally, the Sm phase is a lamellar structure whose translational symmetry is broken in the direction of $\hat{\mathbf{n}}$, and the rods are free to diffuse inside each layer as in a two-dimensional liquid [30]. By contrast, the diffusion from layer to layer is hampered by transient cages and permanent barriers, as recently investigated by theoretical [31], experimental [32], and computational [7,8] works.

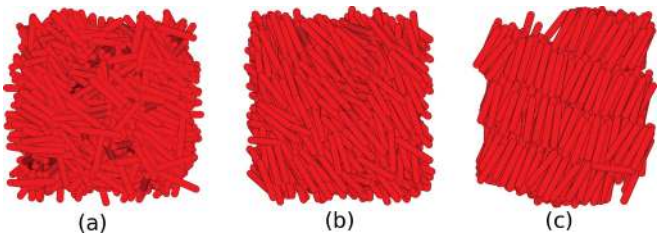

FIG. 1. (Color online) Isotropic (a), nematic (b), and smectic (c) phases of rod-like particles with length-to-diameter ratio $L^* = 5$ and reduced temperature $T^* = 20$, 5, and 3, respectively. The packing fraction is $\eta = 0.490$ for the isotropic and nematic phases, and $\eta = 0.556$ for the smectic phase.

In Figs. 2–4, we show the mean square displacements (MSDs) of rod-like particles in the I, Nm, and Sm phases, respectively. Due to the homogeneous spatial distribution in the I phase, we only calculate the total MSD, defined in Eq. (20). On the other hand, for the Nm and Sm phases, we also report the MSDs perpendicular, $\langle \Delta \mathbf{r}_\perp^2(t) \rangle$, and parallel, $\langle \Delta \mathbf{r}_\parallel^2(t) \rangle$, to the nematic director $\hat{\mathbf{n}}$. For each system, the time was rescaled by applying Eq. (8) with the acceptance rates listed in Table I. Additionally, the MSDs calculated by DMC simulations with not rescaled MC time are also plotted in Fig. 2. As a general tendency, rescaling the MC time produces a very good agreement between the MSDs calculated with the two simulation techniques. Such an agreement is excellent at very low time steps and still very good at $\delta t_{\mathrm{MC}}/\tau > 10^{-2}$, when the acceptance rates become significantly smaller as well as the accuracy of Eq. (8). In the inset of each figure, a double linear scale helps to distinguish the deviations between the rescaled MSDs obtained with DMC and BD simulations. We observe that all the rescaled results of the MSD collapse on a single master curve, which confirms the existence of a single time

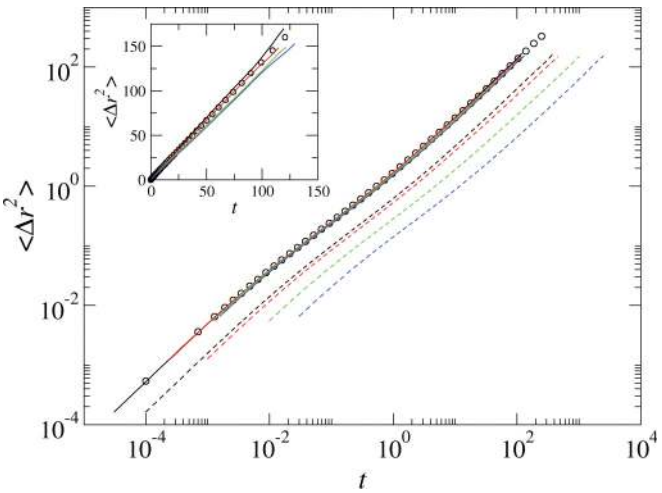

FIG. 2. (Color online) Mean square displacement (MSD) in the isotropic phase of rod-like particles. The empty circles indicate the MSD obtained from BD simulations, whereas the black (upper), red, green, and blue (lower) dashed lines refer to the results from DMC simulations at times $\delta t_{\mathrm{MC}}/\tau = 10^{-4}$, 10^{-3}, 10^{-2}, and $3 \cdot 10^{-2}$, respectively. The solid lines are the same MSDs from DMC simulations with the time rescaled according to Eq. (8). Note the double linear scale of the inset.

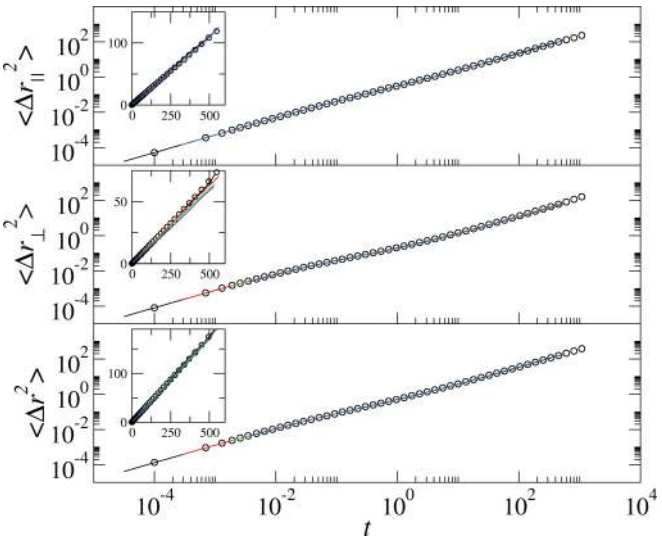

FIG. 3. (Color online) Mean square displacement (MSD) in the nematic phase of rod-like particles in the direction parallel (top frame) and perpendicular (middle frame) to the nematic director. In the bottom frame, the total MSD is also given. The empty circles indicate the MSD obtained from BD simulations, whereas the black (upper), red, green, and blue (lower) lines refer to the results from DMC simulations at times $\delta t_{\rm MC}/\tau = 10^{-4}$, 10^{-3}, 10^{-2}, and $3 \cdot 10^{-2}$, respectively, with the time rescaled according to Eq. (8). Note the double linear scale of the insets.

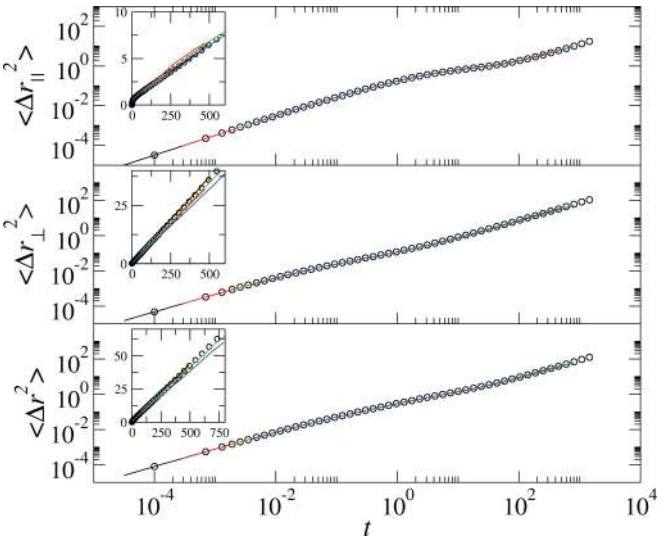

FIG. 4. (Color online) Mean square displacement (MSD) in the smectic phase of rod-like particles in the direction parallel (top frame) and perpendicular (middle frame) to the nematic director. In the bottom frame, the total MSD is also given. The empty circles indicate the MSD obtained from BD simulations, whereas the black (upper), red, green, and blue (lower) lines refer to the results from DMC simulations at times $\delta t_{\rm MC}/\tau = 10^{-4}$, 10^{-3}, 10^{-2}, and $3 \cdot 10^{-2}$, respectively, with the time rescaled according to Eq. (8). Note the double linear scale of the insets.

scale with physical consistency. At $\delta t_{\rm MC}/\tau = 3 \cdot 10^{-2}$ (solid blue curves in Figs. 2–4), the deviations of the rescaled MSDs from the master curve become more evident, although their behavior is still more than satisfactory. The parallel MSDs in the Sm phase show the three typical time-dependent regimes observed in previous works [7,8], where the formation of an intermediate plateau, due to the trapping cage effect of the particles surrounding each other and to the periodic permanent barriers due to the layered arrangement, slows down the motion of the rods and signs the crossover between the short- and long-time diffusive regimes. This effect is captured by both BD and DMC simulations. On the other hand, in the Nm and I phases, the shape of the MSD is that typically observed in fluid-like systems, where the particles enter the diffusive regime in a very short period of time, and no relevant change in the slope of the MSDs is observed.

In Fig. 5, the orientation auto-correlation functions, $E_2(t)$, as calculated from Eq. (21), are given. As expected for liquid crystal phases, where the structural order forces the particles to keep a quasi-aligned orientation, these functions do not decay to zero but saturate to a finite value, which is roughly 0.5 in the Nm phase of Fig. 5(b), and 0.9 in the Sm phase of Fig. 5(c). On the other hand, $E_2(t)$ decays to zero in roughly five time decades in the I phase. Rescaling the results of DMC simulations gives an excellent agreement with the output of BD simulations for the three phases of interest.

Finally, in Fig. 6, we study the long-time relaxation dynamics by computing the ISFs at the wave vectors $\mathbf{q}$, $\mathbf{q}_\parallel$, and $\mathbf{q}_\perp$, corresponding to the first peak of the static structure factor in the three spatial directions and along those parallel and perpendicular to the nematic director, respectively. More specifically, in both Nm and Sm phases, we find $|\mathbf{q}_\parallel| \simeq 1$ and $|\mathbf{q}| \simeq |\mathbf{q}_\perp| \simeq 6$; whereas, in the I phase, the ISF is only calculated at $|\mathbf{q}| = 6$. The relaxation dynamics in the I phase and in the direction perpendicular to $\hat{\mathbf{n}}$ in the liquid crystalline phases, is relatively fast with the ISFs decaying to zero between three and four time decades. On the other hand, the motion of the rods along the direction of $\hat{\mathbf{n}}$ is much slower, especially

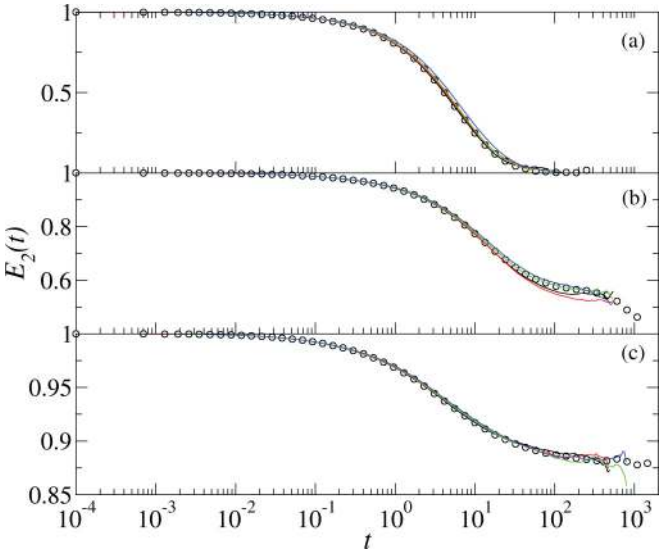

FIG. 5. (Color online) Orientation auto-correlation functions, $E_2(t)$, in the isotropic (a), nematic (b), and smectic (c) phases of rod-like particles. The empty circles refer to BD simulations, whereas the solid lines are the results from DMC simulations at times $\delta t_{\rm MC}/\tau = 10^{-4}$, 10^{-3}, 10^{-2}, and $3 \cdot 10^{-2}$, with the time rescaled according to Eq. (8).

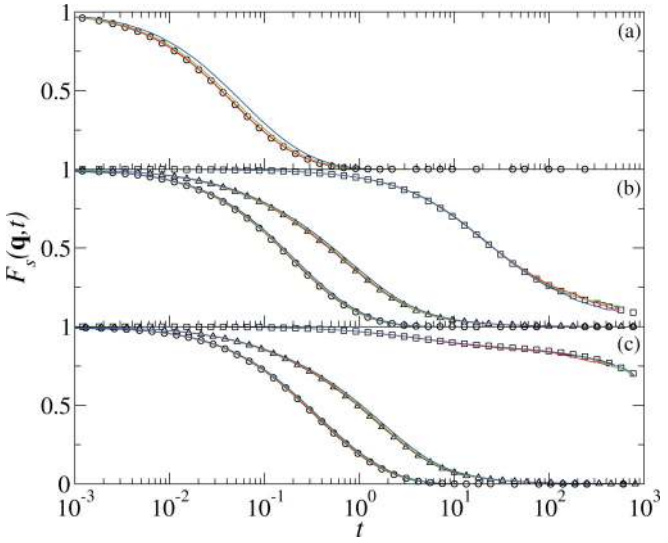

FIG. 6. (Color online) Self-intermediate scattering functions, $F_s(\mathbf{q},t)$, in the isotropic (a), nematic (b), and smectic (c) phases of rod-like particles. All the open symbols are results from BD simulations. Circles refer to the total ISF, whereas triangles and squares, in frames (b) and (c), refer to the parallel and perpendicular directions, respectively. Solid lines are the results from DMC simulations at $\delta t_{\mathrm{MC}}/\tau = 10^{-4}$, 10^{-3}, 10^{-2}, and $3 \cdot 10^{-2}$, with the time rescaled according to Eq. (8).

in the Sm phase, where the formation of a plateau, similar to that observed in the MSDs above, delays the relaxation of the system well beyond our simulation time. The agreement between DMC and BD simulations is again remarkably good, with a slight discrepancy in the I phase for $\delta t_{\mathrm{MC}}/\tau = 3 \cdot 10^{-2}$. At this time step, the acceptance rate is exceptionally low ($\mathcal{A} = 0.157$; see Table I) and it is reasonable to expect some quantitative deviations from the BD results. All the remaining time-rescaled DMC curves of Fig. 6, where $\mathcal{A}$ is above 0.3, don't show any significant difference, apart from small statistical fluctuations, with the corresponding curve obtained from BD simulation.

V. CONCLUSIONS

In summary, in this work we propose a dynamic Monte Carlo approach to estimate the dynamic observables of a system as equivalently obtained by performing Brownian Dynamic simulations. In order to perform a comparative analysis between DMC and BD simulations, we have investigated the dynamics of isotropic phases, and nematic and smectic liquid crystals, containing merely repulsive rod-like colloidal particles interacting via a shifted and truncated Kihara potential. In DMC simulations, the particles are displaced and rotated simultaneously, and the attempted moves are accepted or rejected according to the standard Metropolis algorithm. The DMC trajectory yields to an acceptance rate whose value strictly depends on the MC time step, which in turn determines the maximum displacement and rotation allowed to each particle along the simulation run, as established by the Einstein relation. By rescaling the MC time with the acceptance rates, each of the dynamic properties computed by performing DMC simulations at different time steps collapses into a single master curve, confirming the existence of a unique MC time scale. These curves overlap the corresponding results obtained with BD simulations, showing a very good agreement between the two simulation techniques, especially at high acceptance rates or, equivalently, at low MC time steps. Since rotations and displacements are performed simultaneously in DMC simulations, only one value of the acceptance rate is produced and no preliminary simulations are needed to tune their maximum values. The dynamic behavior in the three phases of interest has been analyzed by the computation of the mean square displacement, orientation auto-correlation functions, and self-intermediate scattering functions. We observed a very good qualitative and quantitative agreement between the results as computed by performing DMC and BD simulations. In particular, both simulation approaches are able to describe the physics of rod diffusion in the nematic and smectic liquid crystalline phases, where the motion in the direction of the nematic director and that perpendicular to it present significant differences.

The DMC method proposed in this work is in principle applicable to any kind of systems containing particles with orientational degrees of freedom, such as platelets, patchy colloids, or other anisotropic particles. In any case, our algorithm presents some restrictions that should be pointed out. First, it is strictly valid only for stationary situations, where the acceptance ratio, apart from reasonable oscillations due to thermal fluctuations in the system, can be assumed to be constant along the whole simulation. Therefore, to investigate the dynamics of out-of-equilibrium systems, a time-dependent acceptance rate should be used to rescale the MC timescale to the BD time. Second, Eq. (6) cannot be straightaway applied to systems containing polydisperse particles (in shape and/or size) or to inhomogeneous systems. Further work is required to extend our results to these particular cases. Taking into account these considerations, the algorithm presented in this work, which partially extends and completes that proposed by Sanz and Marenduzzo in Ref. [18], represents an efficient computational tool to qualitatively and quantitatively address the dynamics of those systems where performing Brownian dynamic simulations might introduce additional difficulties.

ACKNOWLEDGMENTS

A.P. acknowledges Juan de la Cierva Grant No. JCI-2010-06943 from the Spanish Ministry of Science and Innovation (MICINN) and Beatriu de Pinós Grant No. 2009-BP-B00058 from AGAUR. A.C. acknowledges funding from the Operative Programme FEDER-Andalucia 2007–2013 through Project No. P09-FQM-4938 and from Spanish Ministry of Science and Innovation (MICINN) through Project No. MAT2011-29464. Both authors acknowledge Eduardo Sanz for a critical reading of the manuscript.

APPENDIX: BALANCE IN DYNAMIC MONTE CARLO

For a MC algorithm to be valid, it is important to ensure that, at the equilibrium, the distribution function remains stationary. In most of these algorithms, this requisite is satisfied by

imposing the detailed-balance condition, summarized by the following equation:

$$P_i \Pi_{i,j} = P_j \Pi_{j,i}, \tag{A1}$$

where P_i represents the probability to find a system in state i and $\Pi_{i,j}$ the transition probability from state i to state j [4]. The transition probability is usually factorized in two terms, $\Pi_{i,j} = \alpha_{i,j} acc_{i,j}$, where $\alpha_{i,j}$ is the probability to generate a new state j from i, whereas $acc_{i,j}$ is the probability to accept j as a new state.

In the present paper, we have proposed a dynamic MC algorithm that mimics the time evolution of the system under Brownian dynamics. An important aspect of the proposed methodology is that it does not ensure the detailed-balance condition, but still results in a correct MC sampling. For the sake of clarity, we first discuss the 2D case of a rod-like particle p confined in a plane. The extension to the more general 3D case is straightforward. In the 2D case, only one perpendicular vector to the orientation of p should be considered to calculate $\delta\mathbf{r}$ and $\delta\mathbf{u}$, being the maximum displacement and rotation allowed, respectively. If the particle moves to the new position $(\delta r_{||}, \delta r_{\perp})$ and simultaneously changes its orientation, the reverse move is not possible and the detailed balance is not satisfied regardless of the attempted displacement and rotation. Nevertheless, it has been shown that for an MC algorithm to be valid, the detailed balance is sufficient but not necessary [33]. A sufficient and necessary condition, usually referred to as a simple balance condition, provides a correct criterion to check the effectiveness of an MC scheme. As we show here, our dynamic MC algorithm satisfies this condition.

The simple balance condition implies that the number of accepted moves from state i to j must be equal to the accepted moves leading the system to i:

$$\sum_j P_i \Pi_{i,j} = \sum_k P_k \Pi_{k,i} \quad \forall i, \tag{A2}$$

where we only have considered transitions with non-null probability. In this equation, we remark that the sums are over states that are generally different, as the complete set of accessible states from i (states j) does not coincide with the set of states from which i is accessible (states k). As the transition probability is normalized, $\sum_j \Pi_{i,j} = 1$. The transition probabilities in the right-hand side of Eq. (A2) can be rewritten as $\Pi_{k,i} = \alpha_{k,i} \mathrm{acc}_{k,i}$. States i accessible from k with $\alpha_{k,i} \neq 0$ are those obtained with a particle rotation lower than the maximum rotation $\delta\vartheta$ defined in Eq. (12). For each of these orientations, all the points inside the rectangle of size $2\delta r_{||} \times 2\delta r_{\perp}$ have the same *a priori* probability to be displaced to position of state i. Similarly, for the more general f-dimensional case, the number of states from which i is accessible is V_Ξ, where V_Ξ is the volume of the hyperprism defined in Sec. II. Therefore, as all the transitions have the same *a priori* probability, $\alpha_{k,i} = 1/V_\Xi$ if i is accessible from k, or zero otherwise. With all of these considerations, Eq. (A2) reads

$$\frac{1}{V_\Xi} \sum_k \frac{P_k}{P_i} \mathrm{acc}_{k,i} = 1 \tag{A3}$$

There are many possible choices for $\mathrm{acc}_{k,i}$. If P_i is the Boltzmann distribution and $\mathrm{acc}_{k,i}$ is defined according to the Metropolis rule, then $P_k/P_i \mathrm{acc}_{k,i} = 1$ and the balance condition is satisfied.

[1] S. Chandrasekhar, Rev. Mod. Phys. **15**, 1 (1943).

[2] R. Brown, in *The Miscellaneous Botanical Works of Robert Brown*, edited by John J. Bennett, Vol. 1 (London, 1866).

[3] M. P. Allen and D. J. Tildesley, *Computer Simulation of Liquids* (Clarendon Press, Oxford, 1987).

[4] D. Frenkel and B. Smit, *Understanding Molecular Simulation: From Algorithms to Applications*, 2nd ed. (Academic Press, New York, 2002).

[5] L. Berthier and W. Kob, J. Phys.: Condens. Matter **19**, 205130 (2007).

[6] L. Pfleiderer, K. Milinkovic, and T. Schilling, Europhys. Lett. **84**, 16003 (2008).

[7] A. Patti, D. El Masri, R. van Roij, and M. Dijkstra, Phys. Rev. Lett. **103**, 248304 (2009).

[8] A. Patti, D. El Masri, R. van Roij, and M. Dijkstra, J. Chem. Phys. **132**, 224907 (2010).

[9] R. Matena, M. Dijkstra, and A. Patti, Phys. Rev. E **81**, 021704 (2010).

[10] S. Belli, A. Patti, R. van Roij, and M. Dijkstra, J. Chem. Phys. **133**, 154514 (2010).

[11] A. Patti, S. Belli, R. van Roij, and M. Dijkstra, Soft Matter **7**, 3533 (2011).

[12] S. Auer and D. Frenkel, Nature (London) **409**, 1020 (2001).

[13] S.-S. Chern, A. E. Cárdenas, and R. D. Coalson, J. Chem. Phys. **115**, 7772 (2001).

[14] A. Dambal and E. S. G. Shaqfeh, J. Chem. Phys. **131**, 224905 (2009).

[15] J. Huang, Y. Wang, and C. Qian, J. Chem. Phys. **131**, 234902 (2009).

[16] V. Yu. Kiselev, D. Marenduzzo, and A. B. Goryachev, Biophys. J. **100**, 1261 (2011).

[17] N. Metropolis, A. W. Rosenbluth, M. N. Rosenbluth, A. H. Teller, and E. Teller, J. Chem. Phys. **21**, 1087 (1953).

[18] E. Sanz and D. Marenduzzo, J. Chem. Phys. **132**, 194102 (2010).

[19] F. Romano, C. De Michele, D. Marenduzzo, and E. Sanz, J. Chem. Phys. **135**, 124106 (2011).

[20] A. Einstein, *Investigations of the Theory of Brownian Movement* (Dover, New York, 1956).

[21] D. S. Lemons, *An Introduction to Stochastic Processes in Physics* (The Johns Hopkins University Press, Baltimore, 2002).

[22] A. Cuetos, B. Martínez-Haya, L. F. Rull, and S. Lago, J. Chem. Phys. **117**, 2934 (2002).

[23] A. Cuetos, B. Martínez-Haya, S. Lago, and L. F. Rull, J. Phys. Chem. B **109**, 13729 (2005).

[24] C. Vega and S. Lago, Comput. Chem. **18**, 55 (1994).
[25] H. Löwen, Phys. Rev. E **50**, 1232 (1994).
[26] F. Perrin, J. Phys. Radium **5**, 497 (1934).
[27] H. Shimizu, J. Chem. Phys. **37**, 765 (1962).
[28] H. Pei, S. Allison, B. M. H. Haynes, and D. Augustin, J. Phys. Chem. B **113**, 2564 (2009).
[29] C. Vega and S. Lago, J. Chem. Phys. **93**, 8171 (1990).
[30] P. G. de Gennes and J. Prost, *The Physics of Liquid Crystals*, 2nd ed. (Clarendon Press, Oxford, 1993).
[31] M. Bier, R. van Roij, M. Dijkstra, and P. van der Schoot, Phys. Rev. Lett. **101**, 215901 (2008).
[32] M. P. Lettinga and E. Grelet, Phys. Rev. Lett. **99**, 197802 (2007).
[33] V. I. Manousiouthakis and M. W. Deem, J. Chem. Phys. **110**, 2753 (1999).